*Friction* **11**(4): 617–634 (2023)
https://doi.org/10.1007/s40544-022-0629-2
ISSN 2223-7690
CN 10-1237/TH

RESEARCH ARTICLE

# Stable oral lubrication enhancer obtained from thiolated polyethylene glycol and mucin

**Xiaoyan HE**[1,2], **Pravin SMART**[1], **Mohamad TAUFIQURRAKHMAN**[1], **Chun WANG**[1], **Michael BRYANT**[1,*]

[1] *Institute of Functional Surfaces, School of Mechanical Engineering, University of Leeds, Leeds LS2 9JT, United Kingdom*

[2] *Reliability Engineering Institute, National Engineering Research Center for Water Transport Safety, Wuhan University of Technology, Wuhan 430063, China*

*Received:23 October 2021 / Revised: 19 December 2021 / Accepted: 01 April 2022*



**Abstract:** Mucins are vital components contributing to the unique lubrication properties of human whole saliva. For patients receiving medication and or treatment such as diabetes or radiotherapy, xerostomia (dry mouth) is a common with numerous and deleterious side effects. Although products exist on the market to relive the symptoms of Xerostomia there remains a drive to formulate a biocompatible lubricant that replicate the functionality offered by the natural biological environment. Herein, a combination of mucin and thiolated polyethylene glycol (PEG-SH) was proposed as a new saliva substitute. Mucin and PEG-SH molecules could form hydrated layers immediately by chemisorption. Meanwhile, the chemical interactions between mucin and PEG-SH molecules also promoted the formation of a mixed layer. All the pre-formed layers could decrease friction and had the potential to decrease wear, especially mucin and PEG-SH mixed layer when compared to mucin only solutions. Further investigations of tribological mechanism implied that the excellent lubrication performance of mixed layer with long effectiveness was contributed to the friction-reducing effect of PEG/mucin molecules and the mucoadhesive property of mucin. The study provides a guide for using mucin as a mucoadhesive agent to stable lubricative polymers with low molecular weight as novel salivary substitutes for lubrication.

**Keywords:** lubrication; mucin; polyethylene glycol; mucoadhesive; chemisorption

## 1 Introduction

Xerostomia clinically complained as “dry mouth” has negative impacts in approximately 20% of the general population, especially in older people [1]. Xerostomia leads to serious problems in speaking and eating. It also increases the risks of dental complications and malnutrition [2]. Due to the increase in the global aging population, xerostomia is becoming a more prevalent health burden [3]. Therefore, it is important to develop effective therapies that aim to reduce or relieve the uncomfortable symptoms caused by xerostomia.

The most common strategies for dry mouth therapies are the employment of saliva substitutes [4–6]. Saliva is constituted of 98.5%–99% water, 0.2% inorganic and trace element, and 0.3% proteinaceous compounds including mucin, amylases, and other low molecular weight proteins [2, 7, 8]. The proteinaceous compounds immediately adsorb onto a tooth surface to self-assemble a salivary pellicle. This can act as a lubricant to provide excellent lubrication and decrease friction and wear in the mouth [9]. Among these, mucins are the key components to obtain effective boundary lubrication performance [10–12]. Their chemical complexity is responsible for their lubrication properties. The non-glycosylated domains of mucin molecules are usually composed of charged domains,

* Corresponding author: Michael BRYANT, E-mail: m.g.bryant@leeds.ac.uk

hydrophobic domains, and thiolated groups [13]. The non-glycosylated domains ensure that mucin molecules can form established adhesion via electrostatic interactions, van der Waals forces, hydrophobic forces, or chain entanglement [7]. The thiolated groups, which can form disulfide bridges, could also promote mucin adhesion [13]. Meanwhile, mucin molecules are rich in hydroxyl groups, which can engage via intramolecular and intermolecular hydrogen bonds [13] and promote the formation of a hydration layer. The hydration layer around mucin molecules on the surface can work as a perfect lubrication element.

Generally, mucins purified from porcine stomach mucus are often used within artificial saliva substitutes to give hydrating and lubricating effects in research and development [11]. Unfortunately, these commercial porcine gastric mucins can only provide a temporary lubricative function which is restricted by their poor ability in entrapment of sufficient water [4]. Moreover, commercial porcine gastric mucins can easily lose their ability to lubricate surfaces [11]. They are only effective in specific conditions, such as acidic pH and low ionic strength [4]. Therefore, it is essential to promote the effectiveness of saliva substitutes based on mucins. It is necessary to develop saliva substitutes by more effective combinations of lubricant and additional agents.

Polyethylene glycol (PEG), a non-toxic and biocompatible synthetic material [14], is usually used as a mucoadhesive material in commercial salivary substitutes, which can self-assemble an artificial salivary pellicle [15]. It has been proven that Oasis (PEG 60 hydrogenated and castor oil-based) saliva substitutes presented similar adsorption behavior as human saliva [16]. But, the PEG-hydrogenated castor oil-based saliva substitute, including BT spray, Dentaid Xeros (DX) mouthwash, and GUM Hydral (GH) spray, did not show any significant difference in friction behaviors when compared with water, suggesting that these saliva substitutes lack optimum lubricating effects [3].

However, there are some reports that PEG shows perfect lubricating effects in an aqueous environment [17, 18]. A large number of water molecules surrounded the PEG backbone form a hydration layer. This hydration layer is easy to shear off but difficult to squeeze, which could provide enhanced load bearing capacity, low friction and low wear. PEG solutions have been shown to reduce the wear of ultra-high-molecular-weight polyethylene and promote the longevity of knee joint prostheses [19]. Considering the lubricative properties presented by PEG molecules in an aqueous environment, it is worth utilizing the friction-reducing effect of PEG in a water-based saliva substitute instead of the commercial oil-based substitutes. As mentioned above, the commercial porcine gastric mucins can easily lose their friction-reducing effect [4], when they are not in acidic pH and low ionic strength environment. While the human saliva always shows a pH of 6.6–7.1.

The aim of this study was to investigate if PEG can be used to enhance the lubrication properties of a mucin-based saliva substitute in a neutral phosphate buffer solution. Therefore, mucin and thiolated PEG (PEG-SH) were employed to explore their synergistic lubrication effect for hard–hard interfaces. The gold substrate as a traditional dental material was used in the study [20, 21]. The adsorption and tribological properties were investigated in detail. A combination of quartz crystal microbalance with dissipation (QCM-D), micro-tribology, and surface characterization methodologies have been employed to directly assess the materials interfaces structure-function relationship. The results of this study provide beneficial insights into the synergy between mucin and PEG for the development of novel artificial saliva substitutes with enhanced lubrication and protection.

## 2 Experimental

### 2.1 Artificial saliva solutions

Commercially available mucin from porcine stomach (PGM Type II, Sigma) and polyethylene glycol (PEG-SH, 4arm-PEG10K-SH, Sigma) were purchased from Sigma-Aldrich and used in the experiment without further purification. Solutions were prepared by dissolving corresponding powders in phosphate buffer solution (PBS). Three kinds of artificial saliva solutions (including 0.1 wt% mucin solution [22], 0.01 wt% PEG-SH solution [23], and 0.1 wt% mucin-0.01 wt% PEG-SH mixed solution) were prepared. These

solutions were used to investigate the role of mucin molecules and PEG-SH molecules in reducing oral friction, which could provide guidance on fabricating saliva substitutes.

### 2.2 Formation of pre-adsorbed layers

Quartz crystal microbalance with dissipation (QCM-D, Biolin Scientific/Qsense, Sweden) was used to monitor the adsorption process of mucin or PEG-SH molecules. Gold (Quartz PRO, QCM5140TiAu120-050-Q) sensors were used in the experiment. Before their use, the sensors were washed by sonication in MilliQ water for 10 min and then dried by a nitrogen gas flow at room temperature. The cleaned Au sensors were immediately put into the sensor cell.

First, MilliQ water was supplied into the sensor cell to get a stable baseline. Then, the artificial saliva solution was introduced into the sensor cell with a flow rate of 400 μL/min and the adsorption process was monitored for 60 min. After the growth phase, PBS was introduced into the sensor cell to remove the un-adhered macromolecules with rinsed times of 10 min. For comparison, 0.1 wt% mucin, 0.01 wt% PEG-SH, and 0.1 wt% mucin-0.01 wt% PEG-SH mixed solutions were used for layer growth. The formation processes of the PEG-SH/mucin layer and mucin/PEG-SH layer were also recorded via a layer-by-layer method [24]. For example, the PEG-SH/mucin layer was rinsed by 0.01 wt% PEG-SH for 60 min, PBS for 10 min, 0.1 wt% mucin for 60 min, and PBS for 10 min in sequence. The sensor's surfaces were submerged in each macromolecule solution for 60 min. All the processes were performed at a temperature of 25 °C [3, 6, 24].

### 2.3 Morphology of pre-adsorbed layers and substrate surfaces

Atomic Force Microscopy (AFM, Bruker Dimension FastScan™, Germany) was employed to observe the morphology of the pre-adsorbed layers by PeakForce quantitative nanomechanical mapping model (PeakForce QNM) in air conditions. For AFM tests, the sensors with pre-adsorbed mucin, PEG-SH, and their mixed layers were taken out from the sensor cells and then dried by a nitrogen gas flow at room temperature. ScanAsyst-Air cantilevers (Bruker) with a spring constant of 0.3779 N/m was used. Topographic height images were recorded with a scan rate of 0.905 Hz. All images were flattened by the NanoScope analysis software (Bruker).

Post tribological testing (see Section 2.4), vertical scanning interferometry (VSI, NPFlex, Bruker, USA) was used to quantify surface damage of the Au sensors after friction experiments. VSI used white light and surface reflection to obtain the morphology of scratches by a magnification lens of 10×. The whole wear track was analyzed and all the obtained images were stitched together from a three-dimensional (3D) presentation of the surface. The results were analyzed by the Vision64 software (Bruker) to obtain 3D parameters, including length, width, and depth of the scratches, to calculate the total volume loss. To do this, surfaces were scanned and any form or tilt was removed. Volume loss was calculated by estimating missing volume below the fitted origin [5]. Volume loss measurements were conducted on surfaces after being subjected to 700 cycles of sliding.

### 2.4 Friction experiments

The friction behaviors of Au sensors with the pre-adsorbed layers were measured by a microtribometer (NTR$^3$, Anton Paar, UK). The setup was used in a ball on a flat configuration, which was performed in solution against a Ø3 mm yttria-stabilized tetrahedral zirconia polycrystalline (*Y*-TZP) ball. Before the friction experiment, the *Y*-TZP ball was sequentially washed with acetone, ethanol, and deionized water and subsequently dried by a nitrogen gas flow.

Friction forces ($F_t$) were spatially resolved under piezo-controlled actuation across a variety of normal loads ($F_n$). This enabled the assessment of the load dependent frictional responses for the Au and pre-adsorbed layer surface to be determined. The nominal $F_n$ loads of 200–500 μN were applied with an increase of 50 μN every 100 cycles. The sliding amplitude ($\delta$) was 1,000 μm with a constant sliding speed of 3 mm/s. All the tests were performed at room temperature. A calibrated cantilever (ST-S 231, Anton Parr) with $F_n$ stiffness: 0.4808 mN/μm and $F_t$ stiffness: 1.1399 mN/μm was used in the experiment. Under all conditions, $F_t$ was measured with a data acquisition rate of 400 Hz. The $F_t$ vs. $\delta$ loop was used to determine

the average $F_t$ per sliding cycle. This was taken as the average of the forward and reverse $F_t$ under steady state, speed independent sliding conditions. The central 20% region of the normalized friction loop was used to calculate the average friction force during sliding, which ensured that the analysis was of dynamic/kinetic friction [5]. The average $F_t$ for the last 50 cycles under all loading conditions was calculated. Two methods were utilized to interrogate the mechanisms of friction. The 'system average' coefficient of friction ($\mu_{sa}$) was determined by the gradient of average steady state $F_t$ vs $F_n$ curve according to Eq. (1) as

$$F_t = \mu_{sa} F_n + F_o \quad (1)$$

where, $F_o$ is an unknown interfacial adhesion force [25–27]. This provides an average coefficient of friction for a tribology system over a range of loading conditions but may not enable to determine any small changes in coefficient of friction under applied normal load.

To further examine the role of normal load on the lubrication properties of the adsorbed layers, the instantaneous cycle average coefficient of friction ($\mu_{ca} = \frac{F_t}{F_n}$; final 50 cycles) vs applied $F_n$ was observed. This enabled the film's coefficient of friction response at specific normal loads to be examined and any sensitivity to applied normal load observed.

To compare the difference induced by the as-prepared artificial saliva solutions, the friction tests were performed on the Au sensors with the pre-adsorbed layers prepared as Section 2.2 in their corresponding saliva substitutes, respectively. Since it is impossible to continue adding saliva substitutes, they may be replaced by liquids that people drink. Therefore, it is important to investigate the stability of saliva substitutes by testing the friction behaviors of the pre-formed layers after being rinsed by PBS. The friction experiments were also performed in PBS on the sensors with pre-adsorbed layers after being rinsed by PBS for 120 min. To expound the role of mucin or PEG-SH molecules in the lubricant function of the mixed solution, the friction tests were performed on the Au sensors with the pre-adsorbed PEG-SH/mucin and mucin/PEG-SH layers, which were prepared according to Section 2.2.

## 3 Results and discussion

### 3.1 Adsorption process of macromolecules

#### 3.1.1 *Adsorption of bulk lubricants*

QCM-D is a quantitative and sensitive approach to assessing the adsorption properties of molecules, which can provide abundant information about adsorbed layer properties, surface phenomena, and quantitative information of the adsorbed film on the surface of the QCM-D sensor in real-time [15]. The adsorption processes of different artificial saliva substitute solutions to Au sensor surfaces were monitored by QCM-D (Fig. 1). The incubation of MilliQ water resulted in horizontal baselines of frequency shift ($\Delta f$) and dissipation shift ($\Delta D$). With artificial saliva substitute solutions introduced, a rapid decrease in $\Delta f$ and an increase in $\Delta D$ occurred. The adsorption kinetics were dependent on the solution types. The adsorption of mucin molecules could quickly reach a plateau in 5 min. It also presented the minimum decrease in $\Delta f$ out of the three solutions, indicating the lowest adsorption of mucin molecules. Noteworthily, the adsorption of PEG-SH molecules showed the maximum decrease in $\Delta f$, but it took about 30 min to reach equilibrium. Compared with the adsorption of mucin molecules, the curve shape for the adsorption process in PEG-SH and mucin mixed solution was similar, but it showed a larger decrease in $\Delta f$ and a bigger increase in $\Delta D$. An explanation for this is that the agglomerations of mucin and PEG-SH molecules influence the interaction between molecules and Au substrates.

Subsequently, a rinsing step by PBS was represented to remove the unbounded protein/polymer molecules. For the mucin layer and mixed layer, obvious increases in $\Delta f$ and decreases in $\Delta D$ were observed (Figs. 1(a) and 1(c)), indicating that some mucin molecules were removed by PBS. But for the PEG-SH layer, the changes in $\Delta f$ and $\Delta D$ were very slight, indicating the adsorption of PEG-SH was stable. The slight decreases in dissipation for mucin layer and mixed layer indicated that the adsorbed layers formed on the substrates for

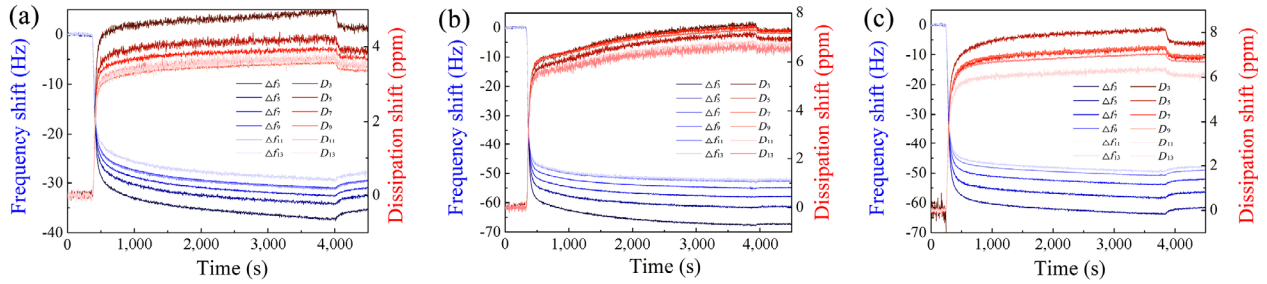


**Fig. 1** Changes in frequency shift ($\Delta f$) and dissipation shift ($\Delta D$) versus time in the formation process of (a) mucin, (b) PEG-SH, and (c) their mixed layers. The shifts in frequency ($\Delta f$) and dissipation ($\Delta D$) at 3rd to 13th overtones were taken into account for analyzing.

all the experimental solutions, but the layers after the rinsing step were more rigid than the initial ones [21].

The plots showing dissipation shift ($\Delta D$) versus frequency shift ($\Delta f$) were further investigated to give a deeper understanding of the structural and viscoelastic properties of the adsorbed layers (Fig. 2). The value of the ratio between $\Delta D$ and $\Delta f$ implies information about viscoelastic properties [21]. A lower value of $|\Delta D/\Delta f|$ results in a stiffer layer. Conversely, a higher value of $|\Delta D/\Delta f|$ leads to a more viscous layer, which provides a better lubricity [21]. The $|\Delta D/\Delta f|$ values of 5th overtone curves were used for analysis. For the formation process of the mucin layer, the curve showed an evident two-regime nature (Fig. 2(a-1)). In the initial growth phase, the sharp decrease in $\Delta f$ and obvious increase in $\Delta D$ with a $|\Delta D/\Delta f|$ value of 0.134 ± 0.004 ppm/Hz suggested the quick formation of the mucin layer (Fig. 2(a-1)). In the second growth phase, the decrease in $\Delta f$ and the slight increase in $\Delta D$ with a $|\Delta D/\Delta f|$ value of 0.124 ± 0.002 ppm/Hz indicated that the formation of mucin layer became slower and less viscous (Fig. 2(a-1)). It can be explained that the adsorption of mucin molecules usually results in two layers with different densities: a viscous part close to the substrate surface and a less viscous part to the solution phase [21, 28]. This phenomenon is similar to the adsorption of a salivary pellicle, which is usually a two-layer structure. After the rinsing step, some unbound mucin molecules were removed, resulting in a minor increase in $\Delta f$. Meanwhile, there was a slight decrease in the $|\Delta D/\Delta f|$ value after rinsed phase (Fig. 2(a-2)). It indicated that the mucin layer was stiffer in PBS than in a mucin solution (Fig. 2(a-2)).

A two-regime formation process was observed with the PEG-SH layer (Fig. 2(b-1)). $|\Delta D/\Delta f|$ values

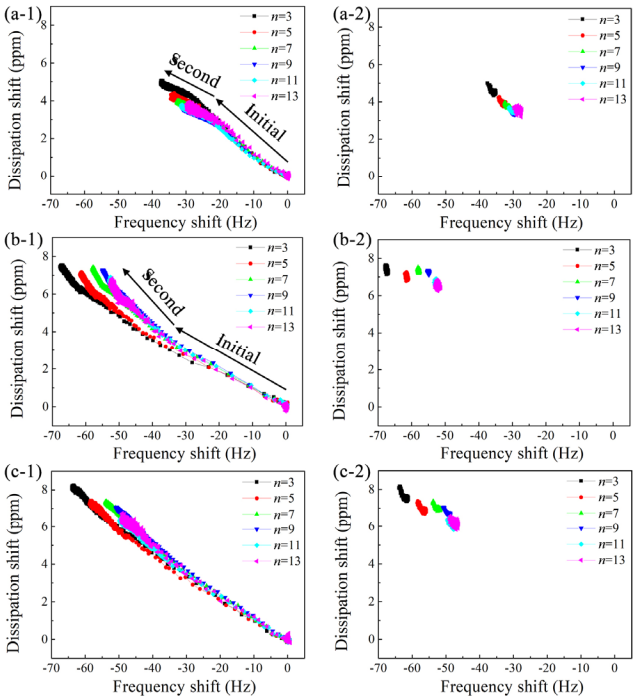


**Fig. 2** $\Delta f$ versus $\Delta D$ curves for the formation process of (a) mucin, (b) PEG-SH, and (c) their mixed layers in their growth phase (-1) and rinsed phase (-2).

were lower at the beginning and then increased. The rapid decrease in $\Delta f$ and obvious increase in $\Delta D$ occurred at the initial stage, indicating the rapid adsorption of PEG-SH molecules (Fig. 2(b-1)). Afterward, there were mild changes in $\Delta f$ and $\Delta D$ indicated by the dense points, where adsorption of PEG-SH molecules reached a plateau (Fig. 2(b-1)). Compared with the $|\Delta D/\Delta f|$ value of 0.105 ± 0.001 ppm/Hz in the initial growth phase, the higher $|\Delta D/\Delta f|$ value of 0.115 ± 0.001 ppm/Hz in the second growth phase indicated the formed PEG-SH layer became more viscous (Fig. 2(b-1)). The adsorption of PEG-SH also resulted in a two-layer structure, but with different

viscosity: a stiffer part close to the substrate surface and a more viscous part to the solution phase. While, the slight decrease in the $|\Delta D/\Delta f|$ value indicated that the PEG-SH layer was stiffer in PBS than in a PEG-SH solution (Fig. 2(b-2)).

Interestingly, the formation process of the mixed layer presented a nearly linear adsorption regime (Fig. 2(c-1)). As mentioned above, $|\Delta D/\Delta f|$ values in PEG-SH adsorption became higher with time, while $|\Delta D/\Delta f|$ values in mucin adsorption decreased. The constant $|\Delta D/\Delta f|$ values in the mixed layer formation process indicated that PEG-SH and mucin molecules participated in the formation of mixed layer. The decrease in $\Delta D$ and the slight increase in $\Delta f$ suggested that a few of molecules were removed and a less viscous layer formed ($|\Delta D/\Delta f| = 0.121 \pm 0.001$ in PBS versus $|\Delta D/\Delta f| = 0.125 \pm 0.001$ in mixed solution) (Fig. 2(c-2)). The unstable molecules with higher viscosity were removed to result in a less viscous layer. Moreover, the different $|\Delta D/\Delta f|$ values before/after being rinsed by PBS indicated that the mixed layer was also a two-layer structure.

The changes in the resonant frequency and the energy dissipation of the Au sensor were detected simultaneously [21] when the macromolecules were adsorbed onto the sensor. These changes were used to calculate the mass/thickness and viscoelastic properties of the adsorbed layer [21]. Usually, the Sauerbrey relation is suitable for a rigid substance [29], while the Voigt model is for viscoelastic solids [24]. Therefore, a Voigt model (namely the "Smartfit Model") was employed to fit the data by Dfind (Q-Sense, Sweden) software to obtain the mass, thickness, and viscosity properties of pre-adsorbed hydrated layers. The viscosities of water, PBS, mucin, PEG, and mixed solutions are 0.889 ± 0.009, 0.901 ± 0.007, 0.935 ± 0.003, 0.896 ± 0.004, and 0.939 ± 0.009 mPa·s, respectively. These viscosities of solutions were used for the model. The 3$^{rd}$ to 11$^{th}$ overtones were taken into account for data analysis.

Figure 3 shows the calculated parameters of pre-adsorbed layers. The thicknesses of the mucin layer and mixed layer were 20.01 ± 2.71 and 23.40 ± 3.35 nm, respectively. The thicknesses increased to 22.18 ± 2.17 and 25.78 ± 2.58 nm after being rinsed by PBS for 10 min, respectively (Fig. 3(a)). It is

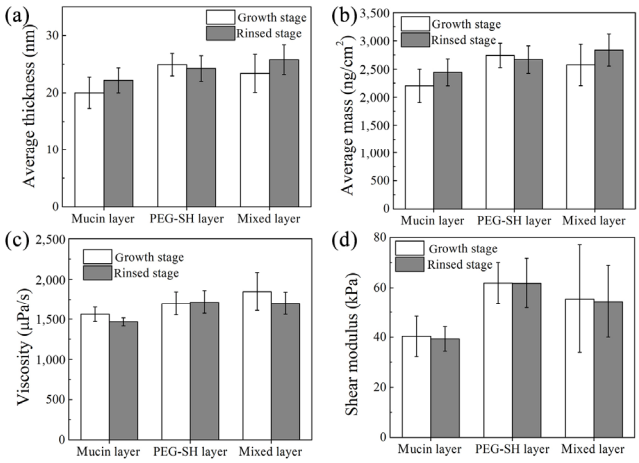


**Fig. 3** (a) Thickness, (b) mass, (c) viscosity, and (d) shear modulus of pre-adsorbed layers (Error bas are shown as ± SD, $n = 5$).

hypothesized that more water molecules were adsorbed on mucin molecules during the PBS rinse. The thickness of the PEG-SH layer was 24.92 ± 1.97 nm and then decreased to 24.24 ± 2.23 nm, which was caused by the removal of the unbound PEG-SH molecules. The obtained thickness values were close to 30 nm, which was the thickness of the saliva pellicle in previous reports [2].

The same phenomenon occurred for masses of the three formed layers (Fig. 3(b)). The masses of mucin, PEG-SH, and mixed layer were 2,201 ± 299, 2,741 ± 216, and 2,573 ± 368 ng/cm$^2$, respectively. The PEG-SH and mixed layers showed higher viscosities (1,697.85 ± 145.99 and 1,846.34 ± 237.91 μPa·s) than that of the mucin layer (1,558.73 ± 89.14 μPa·s) (Fig. 3(c)). After being rinsed by PBS, the viscosity of the mixed layer decreased. The result was in agreement with the observation in $|\Delta D/\Delta f|$ values. Overall, the PEG-SH and mixed layers were thicker and softer compared to the mucin layer. The result was similar to previous studies, where PEG was usually used as an adhesive agent in saliva substitutes to facilitate the formation of a coating [15]. Meanwhile, the PEG-SH and mixed layers showed higher viscosities (61.89 ± 8.16 and 55.56 ± 21.57 kPa) than that of the mucin layer (40.37 ± 8.08 kPa) (Fig. 3(d)). These results also indicate the higher viscoelasticity of the PEG-SH and mixed layers.

The adsorption of macromolecules can usually be explained by three kinds of models: pseudo-first-order (PFO), pseudo-second-order (PSO), and Elovich model, which can provide a deep understanding of

adsorption mechanisms of macromolecules. The PFO model, initially proposed by Lagergren [30], can be written as Eq. (2):

$$q_t = q_e(1-e^{-k_1 t}) \quad (2)$$

In this equation, $q_t$ is the amount of adsorbed molecules onto the substrate in real-time. $q_e$ is the amount of adsorbed molecules at equilibrium. $k_1$ is the rate constant. And $t$ is for the adsorbed time. The PFO model is usually used to describe the process of absorbate onto an adsorbent by physisorption interactions, including hydrogen bonding, electrostatic interactions, van der Waals forces, and hydrophobic interactions.

When the adsorption process is restricted to the active sites in an adsorbent, it is usually described by the PSO model [30], which is proposed by Ho and McKay and written as Eq. (3) [31] as

$$q_t = \frac{k_2 q_e^2 t}{k_2 q_e t + 1} \quad (3)$$

In this equation, $q_t$ and $q_e$ have the same meaning as those in Eq. (2). $k_2$ is the equilibrium rate constant, and the initial adsorption rate could be calculated as Eq. (4) as

$$h = k_2 q_e^2 \quad (4)$$

The PSO model is used to describe chemisorption, where covalent forces and ion exchange play dominant roles in the adsorption process [32]. The valency forces result from the sharing or exchange of electrons between the adsorbent and adsorbate. The PSO model has been successfully used to describe the adsorption of metal ions, dyes, and organic substrates [32].

The Elovich model also describes the chemisorption, which is written as Eq. (5):

$$q_t = \frac{1}{b}\ln t + \frac{1}{b}\ln ab \quad (5)$$

In Eq. (5), $q_t$ is the mass of adsorbed molecules onto the substrate in real-time. The initial adsorption rate is $a$, and the desorption rate is $b$. The equation ignores the interactions between adsorbed molecules.

The mass changes of pre-adsorbed layers versus time were monitored (Fig. 4). The adsorbed masses quickly reached to a plateau. Their initial adsorption stages of 300 s were used to analyze the interaction between molecules and Au surfaces by fitting the three models (Figs. 4(b), 4(d) and 4(f)). The fitting parameters, including $k_1$, $q_e$, $k_2$, and adj $R^2$, were listed in Table 1.

The PSO model was the best fitting for the adsorption process of mucin molecules onto the Au surface in the initial growth phase. Compared with the PFO model, the PSO model fitting presented a higher adj $R^2$ value (0.9948 versus 0.7258) (Fig. 4(b) and Table 1). Moreover, the experimental adsorbed mass of 2,201 ± 299 ng/cm$^2$ was close to 2,030 ng/cm$^2$, which was the calculated mass at equilibrium from the PSO model instead of the PFO model. The perfect fitting of the PSO model suggested that chemisorption played a dominant role in the process of mucin adsorption. Generally, mucin adsorption to surfaces was mediated by physical forces, such as electrostatic and hydrophobic interactions [33]. The thiolated groups in mucin molecules, which could engage in disulfide bridges with the gold surface, could also promote their adhesion [13]. The formation of disulfide

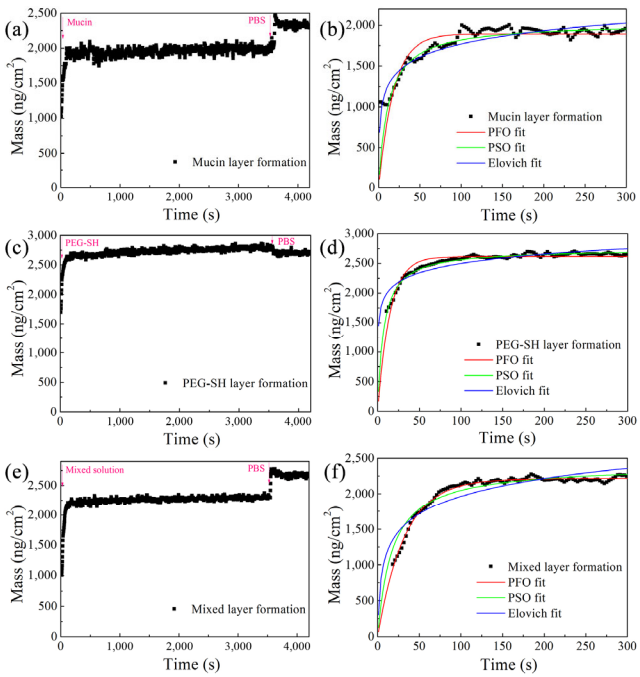


**Fig. 4** (a, c, e) Mass changes of pre-adsorbed layers versus time and (b, d, f) fitting models for the formation process of mucin, PEG-SH, and mixed layers at the initial growth stage.

**Table 1** Fitting parameters in PFO, PSO, and Elovich models for the formation process of mucin, PEG-SH, and mixed layers.

| | PFO | | | PSO | | | Elovich | | |
|---|---|---|---|---|---|---|---|---|---|
| | $K_1$ | $q_e$ | adj $R^2$ | $K_2$ | $q_e$ | adj $R^2$ | $a$ | $b$ | adj $R^2$ |
| Mucin layer | 0.05488 | 1,896 | 0.7258 | $4.259\times10^{-5}$ | 2,030 | 0.9948 | 4,456 | 0.004264 | 0.848 |
| PEG-SH layer | 0.06800 | 2,615 | 0.8875 | $5.089\times10^{-5}$ | 2,745 | 0.9771 | $1.34\times10^{5}$ | 0.004396 | 0.8193 |
| Mixed layer | 0.03069 | 2,214 | 0.9881 | $2.367\times10^{-5}$ | 2,406 | 0.9376 | 840.1 | 0.002776 | 0.7919 |

bridges is typical chemisorption, which can enhance adsorption and contribute to elution resistance.

Meanwhile, the PSO model was also the best fitting for the adsorption process of PEG-SH molecules onto the Au surface in the initial growth phase (adj $R^2$ = 0.9771) (Fig. 4(d) and Table 1). It was indicated that the adsorption of PEG-SH molecules was mainly driven by chemical interaction, such as valance forces through the sharing of electrons between PEG-SH molecules and Au substrates. The –SH functional groups in PEG-SH molecules can form Au–S bonds with the Au surface [34]. The formed Au–S bonds promoted the chemisorption of PEG-SH.

Interestingly, both PFO and PSO models were suitable for mixed layer formation on the Au surface in the initial growth phase (Fig. 4(f)). The adj $R^2$ values for the two models were 0.9881 and 0.9376, which are both close to 1 (Table 1). The PFO model might be a better fitting with a higher adj $R^2$ value than that of the PSO model. However, the calculated mass at equilibrium from the PSO model was 2,406 ng/cm$^2$, which was closer to the experimental adsorbed mass of 2,573 ± 368 ng/cm$^2$ (Table 1). Therefore, the two adsorption interactions could simultaneously occur, suggesting that both chemisorption and physisorption dominated the formation of the mixed layer. Moreover, the initial adsorption kinetics in the PSO model indicated that the formation rate of the mixed layer was slowest. It was speculated that the covalent disulfide bridges between mucin molecules and PEG-SH promoted their mucoadhesion [15]. Covalent force, hydrogen bonds, or electrostatic interaction would also facilitate the mixed layer formation [15]. The result was in agreement with most previous reports that PEG-SH can facilitate the formation of an artificial salivary pellicle [15].

The mass changes and fitting models provided direct information that both mucin and PEG-SH could quickly adsorb onto Au surfaces via chemisorption. Meanwhile, some physical interactions, including electrostatic and hydrophobic interactions, also played roles in mucin adsorption. Interestingly, both chemisorption and physisorption played important roles in the formation of the mixed layer (Fig. 4(f)). The physical interaction in the mixed layer was much more obvious than that in other layers. Maybe it was caused by the interactions between mucin and PEG-SH molecules, which was worth exploring.

### 3.1.2 *Layer-by-layer formation*

To understand the interactions between mucin and PEG-SH molecules, the formation processes of the mucin/PEG-SH and PEG-SH/mucin multilayers formed via layer-by-layer were investigated by QCM-D (Fig. 5). All the curves showed a two-stage film formation process with different mass changes. Focused on the formation of the PEG-SH/mucin layer, the initial adsorption of PEG-SH molecules onto the Au surface was fitted by the PSO model (adj $R^2$ = 0.9771), which had been discussed above (Fig. 4(d) and Table 1). With the PBS rinse, removal of the unbound PEG-SH molecules occurred, which induced a slight decrease in mass. With the subsequent addition of mucin solution, an increase in the layer's hydration mass was observed. The adsorption of mucin molecules onto the formed PEG-SH layer could be fitted by PFO (adj $R^2$ = 0.8981) and PSO (adj $R^2$ = 0.9128) models (Fig. 5(a)). The improved fit of the PSO model suggested that chemisorption played a dominant role in the process of mucin adsorption onto the PEG-SH layer. The chemical interaction of PEG-SH and mucin molecules were promoted by covalent disulfide bridges via thiol groups [15]. After the adsorption of mucin molecules onto the PEG-SH layer, the hydration mass increased from 2,386 to 3,080 ng/cm$^2$ (Fig. 5(a)). However, no obvious difference in their viscosity,

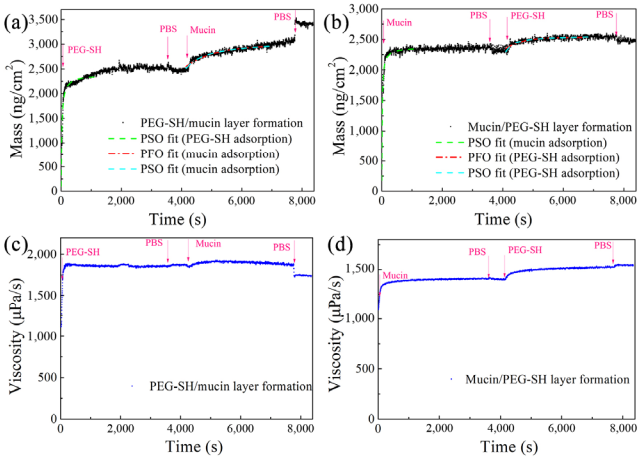


**Fig. 5** Mass changes with their fitting models in the formation process of (a) PEG-SH/mucin and (b) mucin/PEG-SH layers. Viscosity changes in the formation process of (c) PEG-SH/mucin and (d) mucin/PEG-SH layers.

from 1,850 to 1,874 μPa/s (Fig. 5(c)), was observed. The stable viscosities suggest that the adsorption of mucin molecules didn't change the layer structural compositions. Noteworthy, mucin molecules continued adsorbing onto the PEG-SH layer and needed a long time to reach an equilibrium. It can be related to the properties of mucin molecules. The electrostatic and hydrophobic interactions between mucin molecules contribute to their subsequent adsorption.

The formation of the PEG-SH/mucin layer was also investigated (Figs. 5(b) and 5(d)). The adsorption process of PEG-SH molecules onto the formed mucin layer could be fitted by the PSO (adj $R^2$ = 0.9966) instead of the PFO (adj $R^2$ = 0.7319) model, which illuminated the chemical interactions between PEG-SH and mucin molecules (Fig. 5(b)). However, there was an increase in hydration mass (from 2,368 to 2,561 ng/cm$^2$) when compared to mucin films formed in PEG-SH precursor surfaces (Fig. 5(b)). Meanwhile, it was worth noting that the viscosity of the layer continued increasing from 1,400 to 1,530 μPa/s (Fig. 5(d)). It is speculated that PEG-SH molecules continue adsorbing onto the pre-formed mucin layer, while the minor change in hydration mass and the evident change in viscosity are caused by the complex formation of PEG-SH and mucin molecules [24]. PEG-SH molecules may insert or substitute into the pre-adsorbed mucin layer, rearranging the surface distribution of mucin/PEG-SH layer to change its surface viscosity.

The layer-by-layer growth behaviors clarified the interaction between PEG-SH and mucin molecules. The chemical interactions, including covalent disulfide bridges, promoted the adhesion of PEG-SH and mucin molecules [15]. Mucins in saliva substitutes always functioned as lubricating agents in previous studies. While, in this study, mucin was also performed as a mucoadhesive agent, which could facilitate the adhesion of PEG-SH molecules. The investigations further provide evidence that the higher viscosities of layers are mainly contributed to PEG-SH molecules.

### 3.2 Morphology of pre-adsorbed layers

The morphologies of pre-adsorbed layers corresponding to data presented in Section 3.1.1 are shown in Fig. 6. The Au sensor surface showed an initial surface roughness of $R_a$ = 1.47 nm (Fig. 6(a-1)). Therefore, it

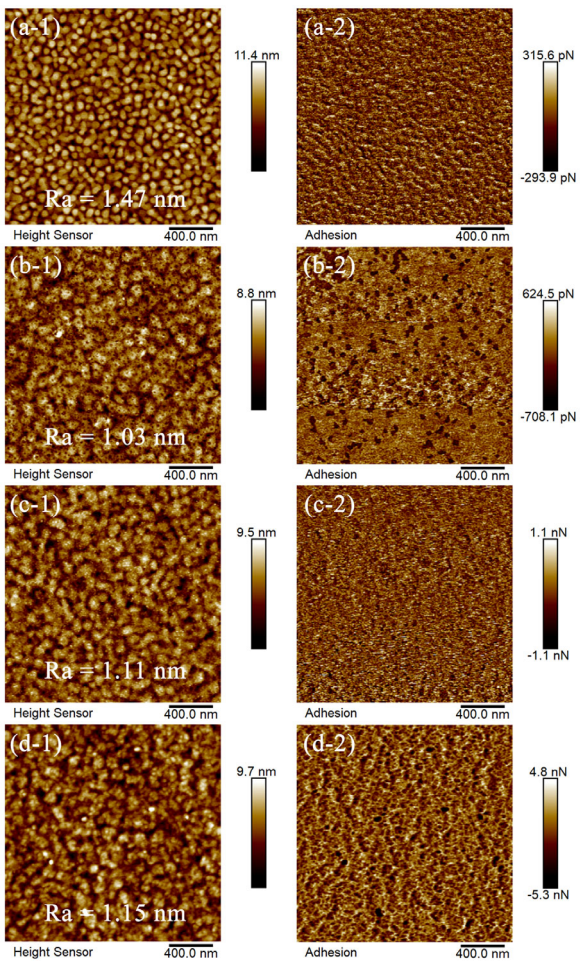


**Fig. 6** AFM height images (-1) and adhesion images (-2) of (a) Au sensor surface and the surface with (b) pre-formed mucin, (c) PEG-SH, and (d) mixed layers.

is difficult to provide quantitative data in height to describe their morphologies. The adsorbed mucin molecules presented a network-structured layer (Fig. 6(b-1)). The formed mucin layer decreased the initial roughness of the Au surface ($R_a$ = 1.03 nm versus $R_a$ = 1.47 nm) (Fig. 6(b-1)), indicating that some mucin molecules adsorbed onto the pores of the Au surface to decrease its roughness. The disulfide bridges, electrostatic and hydrophobic interactions between mucin molecules promoted their adsorption [33]. It was difficult to observe individual mucin molecules since mucin molecules readily formed a three-dimensional network layer since that the sensor was rinsed in the mucin solution for a long time. It is speculated that the empty spaces in the network layer are localized for bound and unbound water to form a highly hydrated matrix in the liquid environment [35]. It also indicates that mucin spreads over the surface to form a highly hydrated matrix in an aqueous environment.

For the PEG-SH layer, there were some small globular structures on the surface (Fig. 6(c)). The width of the globular structures was around 30 nm, indicating individual structures were aggregates of several molecules (Fig. 6(c-1)). The mixed layer was with larger globular structures (Fig. 6(d-1)). The larger size might contribute to the connection of mucin and PEG-SH molecules by chemical interaction (Fig. 6(d-1)). Moreover, the mixed layer also exhibited a network structure that covered the substrate evenly (Fig. 6(d-1)). The adhesion images also directly indicated the formation of different layers (Figs. 6(b-2), 6(c-2), and 6(d-2)). The globular and nanoscaled network structures resulted from the adsorption of mucin/PEG-SH molecules, which could entrap water molecules to give a low friction [4].

### 3.3 Friction behavior of pre-formed layers

The results so far have demonstrated the successful formation of mucin, PEG-SH, and their mixed layer on Au sensors. The sensors with pre-formed layers were suitable to conduct further friction experiments. Fiction behaviors on pre-adsorbed layers in their corresponding solutions were assessed using a microtribometer. 'Growth stage' QCM data presented in Fig. 3 can be linked to this tribological testing. Initial tests were performed on the Au surfaces in a PBS solution without any macromolecule layer, acting as a control group to compare with other formed layers. The friction force ($F_f$) and cycle average coefficient of friction ($\mu_{ca}$) were measured by applying nominal loads ($F_n$) in the range of 0.2–0.5 mN. Subsequent VSI analysis was conducted to further interrogate the durability of the formed films and their ability to protect the underlying substrate.

Figure 7(a) shows a comparative plot of $F_t$ vs. $F_n$ obtained according to the protocol outlined above. In all cases, a nearly linear increase in $F_t$ was observed with increasing $F_n$. For control Au surfaces rinsed with PBS, coefficient of friction was $\mu_{sa}$ = 0.52 ± 0.01. The addition of mucin and PEG molecules decreased the coefficient of friction. The lowest coefficient of

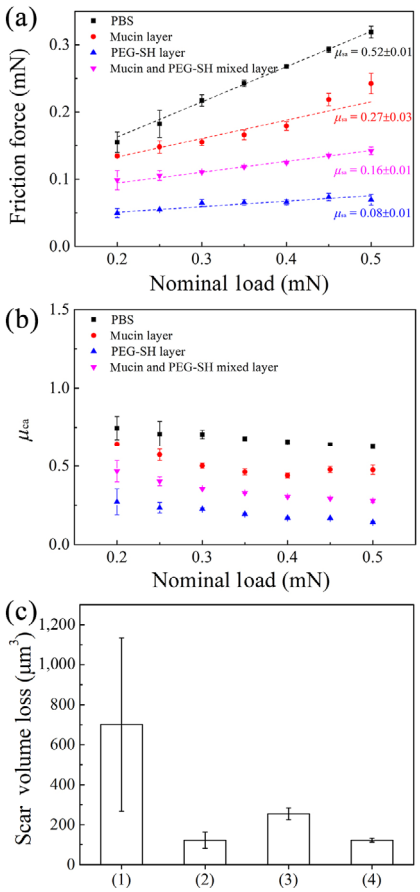


**Fig. 7** Friction force and $\mu_{ca}$ measurements in PBS, mucin, PEG-SH, and their mixed solution on the corresponding pre-adsorbed layer under (a, b) different nominal force and (c) their volume loss: (1) Measurements in PBS, (2) measurements in the mucin solution on the pre-formed mucin layer, (3) measurements in PEG-SH solution on the pre-formed PEG-SH layer, and (4) measurements in the mixed solution on the pre-formed mixed layer.

friction was for the PEG-SH system ($\mu_{sa}$ = 0.08 ± 0.01). Similarly, a decrease in the unknown interfacial adhesion force, $F_o$, was observed, suggesting that the PEG layer may reduce adhesive shear forces at the interface (PBS: 0.058 mN vs. PEG-SH: 0.034 mN). Figure 7(b) shows the instantaneous $\mu_{ca}$ vs. $F_n$. Similar to Fig. 7(a), a reduction in $\mu_{ca}$ was seen with the PEG-SH layer, providing the greatest reduction in friction when compared to the Au control surface. Interestingly, a decrease in $\mu_{ca}$ was observed with increasing load for mucin layers, which may be indicative of hydration lubrication type mechanisms.

Figure 7(c) shows the average volume losses of Au surfaces under different conditions. In all cases, the presence of mucin or PEG layers reduced the total volume loss from the Au surface. However, the sample with the PEG-SH layer showed a higher volume loss than that with mucin/mixed layer, although the friction force was lowest for the PEG-SH system.

Figure 8 shows the correlation between $\mu_{sa}$ and QCM values calculated above. A direct comparison between the layers' viscoelastic properties and system average coefficients of friction has been provided. The coefficient of friction appears to be loosely dependent on layer thickness. A decrease in coefficient of friction with increasing layer viscosity and shear modulus was observed. Yakubov et al. [22] pointed out that the coefficient of friction was related to the viscous stress, which was inversely proportional to the total thickness of the adsorbed layer. In our study, the PEG-SH layer and mixed layer with higher thickness, viscosity and shear modulus resulted in lower friction forces and lower $\mu_{sa}$ (Fig. 8), when compared to the mucin only layers. The friction behaviors on the pre-formed PEG-SH layer in PEG-SH solution with a low viscosity were similar to Sajewicz's research, in which some instability of the tribological characteristics happened in the solution with low viscosity and substantially increased severe wear of enamel [36]. It is speculated that some PEG-SH molecules were removed in the friction process, but could rapidly reabsorb from the bulk solution and continue to form a layer and reduce Au wear.

It is largely agreed that a tightly adhered lubricant layer can promote lubrication [15]. Generally, water is a major component of most aqueous lubrication in nature. However, it is difficult to provide a load-bearing lubricant layer at high pressures and low sliding speeds. Adsorption of PEG-SH molecules showed the decreased $\mu_{ca}$ within the range of loading force. This maybe explained that a hydration layer formed by a large number of water molecules surrounds the adsorbed PEG-SH molecules. In addition, Fig. 7(b) shows a decreasing $\mu_{ca}$ with increasing normal load, which may provide further evidence of a hydration-type lubrication mechanism. It is hypothesized that the hydration layer is responsible for low friction through confinement of hydrated species and fluid pressurization at the interface that enables low shear force to slip between two surfaces [37]. Furthermore, the reduction in interfacial adhesive force suggest that adsorption of mucin and PEG-SH molecules could partially decrease the hydrophobic adhesive forces between tribo-surfaces via a viscous lubrication mechanism.

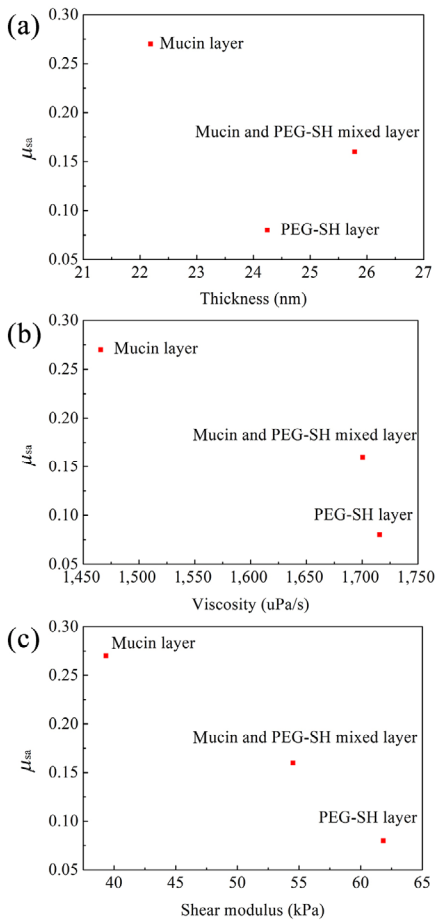


**Fig. 8** Changes in $\mu_{sa}$ versus thickness, viscosity, and shear modulus.

In order to elucidate the stability of pre-adsorbed layers, the friction behaviors were measured on the pre-formed layers after being rinsed by PBS for 120 min. The formation processes of mucin, PEG-SH, and their mixed layers after being rinsed by PBS for 120 min were exhibited (Fig. S1 in the Electronic Supplementary Material (ESM)). Figures 9(a) and9(b) show a comparative plot of $F_t$ vs. $F_n$ (with $\mu_{sa}$) and the instantons cycle average friction ($\mu_{ca}$), respectively. An increase in $\mu_{ca}$ from 0.08 ± 0.01 to 0.27 ± 0.01 was observed for the PEG-SH layer after the 120 minutes PBS rinse when compared to data presented in Fig. 7(a). This lubrication behavior was close to the Au sensor without any layer in PBS. The QCM data (Fig. 4(d) and Table 1) indicated that PEG-SH molecules were adsorbed by chemical interaction, which should provide a stable lubrication effect since covalently bound layers are more robust against wear [22]. However, the PEG-SH layer lost its lubrication effect after being rinsed by PBS for 120 min. It is speculated that the PEG-SH layer with the small globular structures (Fig. 6(c)) is easy to remove by friction since there is no connection between the individual globular structures or may be degraded significantly during the rinse phase. This resulted in a higher $\mu_{ca}$ (Fig. 9(b)) and increased volume loss (Fig. 9(c)). It is important to note that there was no significant increase in the reported $\mu_{sa}$ for the mucin and mixed layer systems after the 120 min PBS rinse. This indicated the films were durable to the PBS rinse compared with the PEG-SH layers. The system average coefficient of friction for the mucin layer was stable ($\mu_{sa}$ = 0.28 ± 0.01 versus 0.27 ± 0.03), as well as the mixed layer ($\mu_{sa}$ = 0.19 ± 0.01 versus 0.16 ± 0.01). The molecules in the mucin layer with a three-dimensional network structure (Fig. 6(b)) and the mixed layer with larger aggregates (Fig. 6(d)), are difficult to remove due to their interactions. The PEG and mucin mixed layer could apply better lubrication effects for a long time. It also resulted in lower volume loss from the Au surface.

Tribology measurements indicated that the PEG and mucin mixed layer could promote better lubrication within an aqueous environment; albeit the long-term durability of PEG-SH only layers was not as effective as the mixed layers. Combining the friction behavior of the PEG-SH layer and the volume losses from Figs. 7 and 9, it is speculated that the small globular PEG-SH molecules can be easily removed from the pre-adsorbed surfaces by sliding or rising. In this case where PEG-SH molecules exist in the solution (Fig. 7), any loosely absorbed molecules removed due to sliding maybe quickly reabsorbed onto the exposed surface (Fig. 10(a)). Thus, $\mu_{ca}$ of the pre-adsorbed PEG-SH layer in its solution can remain at low values despite damage being observed on the Au surface. However, the removal of the loosely absorbed PEG-SH film has occurred by sliding when PEG-SH was not present, replenishment did not occur (Fig. 10(d)), resulting in higher friction and higher Au volume losses. A similar observation can be made for the

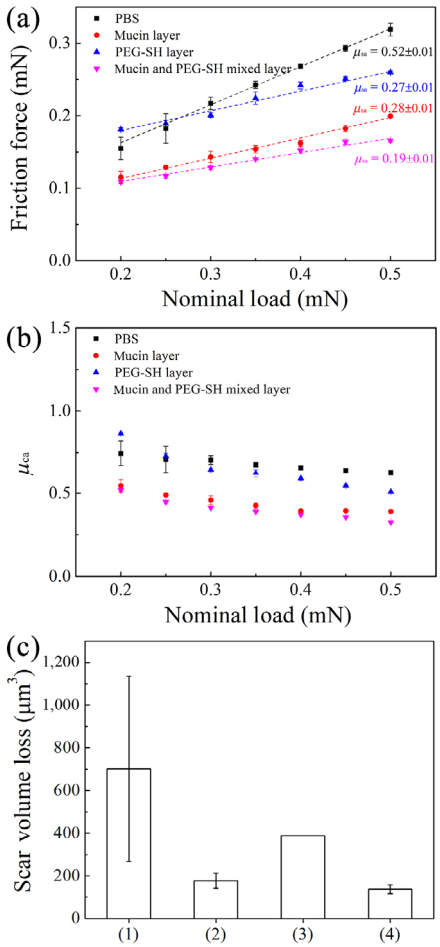


**Fig. 9** (a) Friction force and (b) $\mu_{ca}$ measurements on pre-adsorbed mucin, PEG-SH, and their mixed layer after rinsed by PBS for and 120 min under different nominal forces and (c) their volume loss: (1) Measurements in PBS, (2) measurements on the pre-formed mucin layer, (3) measurements on the pre-formed PEG-SH layer, and (4) measurements on the pre-formed mixed layer.

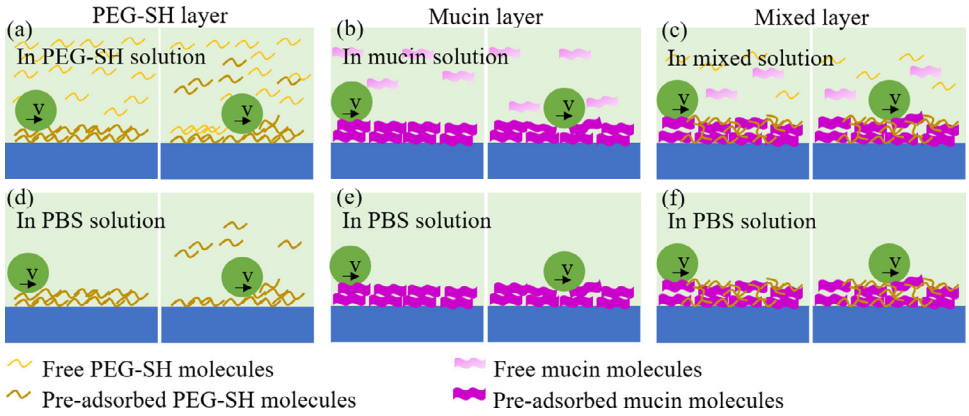


**Fig. 10** Proposed mechanisms of friction behavior under different situation: (a) Measurements on the pre-formed PEG-SH layer in PEG-SH solution, (b) measurements on the pre-formed mucin layer in the mucin solution, (c) measurements on the pre-formed mixed layer in the mixed solution, (d) measurements on the pre-formed PEG-SH layer in PBS, (e) measurements on the pre-formed mucin layer in PBS, and (f) measurements on the pre-formed mixed layer in PBS.

mucin layer. Tribological tests on the mucin layer in PBS solution indicated a slight increase in $\mu_{ca}$ and an increase in Au volume loss, when compared to surfaces slid in the growth solution. This suggests that although mucin may be removed from the surface during sliding, reabsorption may maintain a reduced Au wear. Without a doubt, the durability and ability to decrease Au wear of mucin and mixed layers is due to their complex three-dimensional network structures (Figs. 6(b) and 6(d)) and the chemical interaction between biomacromolecules and Au surfaces (Figs. 4(b) and 4(f) and Table 1). The adhesion force between mucin/mixed layer and the substrate is higher; the adsorbed molecules are difficult to remove and produce a more durable and stable surface layer (Figs. 10(b) and 10(e)). The complex chemical interaction between biomacromolecules and Au surfaces (Figs. 4(b) and 4(f), and Table 1) and the three-dimensional network structures (Figs. 6(b) and 6(d)) are responsible for their stability. It is well established that macromolecular lubrication is sensitive to the environment in which they operate [4]. The data presented in this section highlights the stability of mucin and PEG-SH mixed layers in different lubricant systems (Figs. 10(c) and 10(f)) A similar coefficient of friction and Au volume loss was observed for tests conducted in the growth solution and PBS suggesting that lubricity and Au wear reduction is less dependent on reabsorption processes due to the complex and tightly packed layer structure.

### 3.4 Investigation of friction mechanisms through layer-by-layer assembly

Since the pre-formed mixed layer exhibited lower system and cycle average coefficient of friction, it was worth exploring the dominant element in the lubricant function of the mixed layer: PEG-SH or mucin molecules. The lubricant behaviors of Au sensors with the pre-adsorbed PEG-SH/mucin layer could indicate the role of mucin molecules since that mucin molecules composed the outer layer. Meanwhile, the function of PEG-SH molecules could be illuminated by the lubricant behaviors of the mucin/PEG-SH layers. Therefore, the lubricant behaviors of the PEG-SH/mucin and mucin/PEG-SH layers were investigated to better understand the friction mechanisms of the mucin and PEG-SH mixed layer. Figure 11 shows a comparative plot of $F_t$ vs. $F_n$ with calculated $\mu_{sa}$ and instantaneous $\mu_{ca}$ vs. $F_n$, for pre-adsorbed PEG-SH/mucin and mucin/PEG-SH layers on Au sensors, respectively. Comparing the surface layers developed through a layer-by-layer method, the coefficient of friction for the PEG-SH/mucin layer system was much higher when compared to the mucin/PEG-SH layer (Figs. 11(a) and 11(b)). The PEG-SH molecules in the outer surface of the mucin/PEG-SH layer contributed to lower friction force and coefficient of friction ($\mu_{sa}$ and $\mu_{ca}$). This indicated that PEG-SH played a more important role in anti-friction behavior than mucin molecules, similar to the results in Fig. 7.

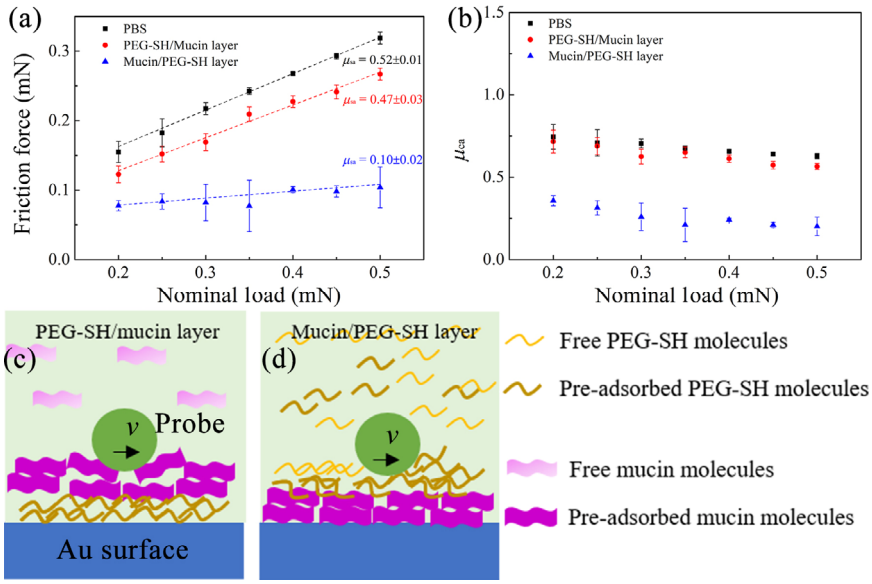


**Fig. 11** (a) Friction force and (b) $\mu_{ca}$ measurements on the pre-adsorbed PEG-SH/mucin and mucin/PEG-SH layer under different nominal forces. The measurement in PBS was used as a reference. The friction mechanisms for (c) PEG-SH/mucin and (d) mucin/PEG-SHlayer system.

The result indicated that PEG-SH contributed to the friction reduction behavior for the pre-formed mixed layer. The PEG-SH layer showed excellent lubrication effect in PEG-SH solution while it easily lost its lubrication effect after being rinsed by PBS for 120 mins (Figs. 7 and 9). The friction tests were performed on the Au sensors with the pre-adsorbed mucin/PEG-SH layer and PEG-SH layer in PBS after being rinsed by PBS for 60 min to explore the role of mucin molecules. Noteworthy, the mucin/PEG-SH layer provided a lower coefficient of friction ($\mu_{sa}$ = 0.11 ± 0.01) than the PEG-SH layer ($\mu_{sa}$ = 0.40 ± 0.01) after the 60 mins PBS rinse (Figs. 12(a) and 12(b)). Combined with the chemical interaction between mucin and PEG-SH molecules (Fig. 5), it was speculated that PEG molecules could interpenetrate into the mucin layer by chemical interaction and diffusion to facilitate mucoadhesion to stabilize themselves, resulting in increased hydration at the interface [18] and then decreased friction (Fig. 12(c)). While, the PEG-SH molecules would be removed from the pre-adsorbed PEG-SH layer when the probe slid from the Au surface, leading to increased friction force (Fig. 12(d)). The result emphasized the mucoadhesion property of mucin molecules.

Moreover, the lubrication of PEG-SH molecules was further clarified by the comparisons of the friction behaviors on the Au sensors with the pre-adsorbed mucin/PEG-SH layer and mixed layer in PBS after being rinsed by PBS for 60 min. Compared with the mucin and PEG mixed layer, the mucin/PEG-SH layer presented lower coefficient of friction under different nominal forces (Fig. 12). It is hypothesized there are PEG molecules in the outer surface of the mucin/PEG layer owing to the better lubrication properties (Figs. 12(c) and 12(e)).

Tribology measurements on different pre-adsorbed layers indicated that the friction-reducing effect of PEG-SH/mucin and the mucoadhesive property of mucin contributed to a better lubrication effect of the mixed layer. PEG-SH and mucin synergistically formed an enhanced macromolecular architecture to decrease friction. Future work will be focused on the enhancement of these systems in terms of lubrication and durability. In this system, both mucin and PEG-SH molecules may contribute to the entrapment of water molecules to provide boundary lubrication. PEG-SH molecules could present a better lubrication effect since PEG-SH molecules could attract higher quantities of water molecules to form a hydration layer to achieve low friction and lower wear. As mentioned before, mucins have been shown to provide enhanced lubrication properties, but they are restricted by specific conditions, such as acidic pH and low ionic

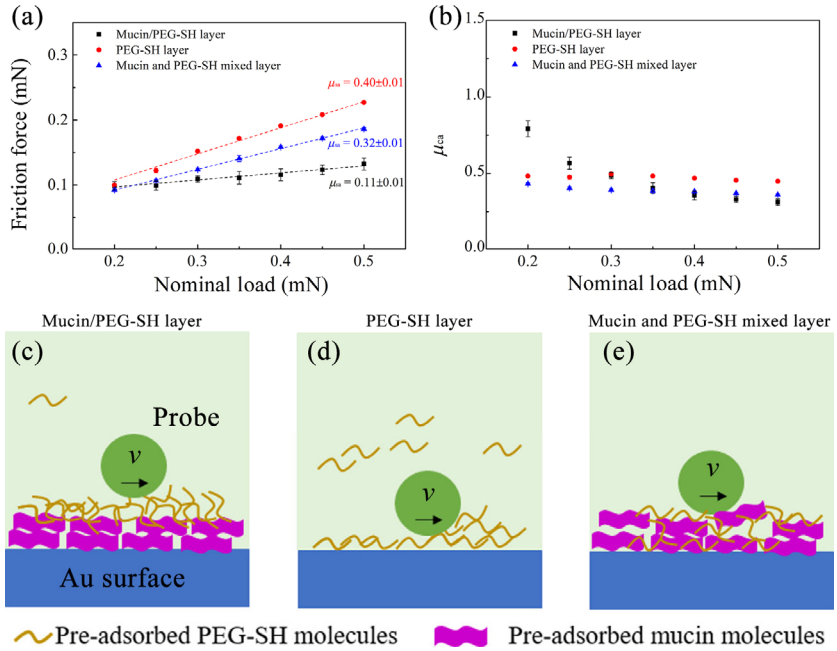


**Fig. 12** (a) Friction force and (b) $\mu_{ca}$ measurements on pre-adsorbed mucin/PEG-SH, PEG-SH, and mixed layer after rinsed by PBS for 60 min. The friction mechanism for (c) mucin/PEG-SH, (d) PEG-SH, and (e) mixed layer in PBS.

strength [4]. In this report, mucins only played a relatively minor role in the lubrication of Au surfaces in PBS when compared to the mucin and PEG-SH mixed layer. It is worth noting that mucin molecules can interact with the surface (Fig. 4(b) and Table 1) to form a robust boundary layer with a three-dimensional network structure (Fig. 6(b)) and act as a cohesion material to enhance the adsorption of PEG-SH (Figs. 5(b) and 5(d)). Therefore, the mucin and PEG-SH mixed layer can provide a better lubrication performance with long effectiveness.

Although the mucin/PEG-SH layer formed by layer-by-layer approach showed a more robust film with similar salivary film properties (Figs. 11 and 12), the practical application and delivery method to the oral cavity needs to be considered. The mixed mucin and PEG-SH solution may represent a more practical application where the molecules are delivered in a single application. In this study, the potential cross-linking of mucin and PEG-SH molecules increase their mixed layer's elasticity and cohesiveness with the potential to improve durability/wear resistance. It presented $\mu_{sa}$ of 0.16 ± 0.01 lubricated by mucin and PEG-SH mixed solution, which was smaller than the $\mu_{sa}$ of 0.27 ± 0.03 lubricated by mucin solution (Fig. 7) and that is currently available as a dry mouth treatment [38]. However, the reported values of a friction coefficient between smooth surfaces lubricated by human saliva are in the range between 0.01 and 0.1 [6], which is smaller than the experimental values in this paper. It is worth adjusting the proportion of mucin and PEG-SH molecules to develop better lubricative saliva substitutes in future work.

### 3.5 Study limitations

Whilst this study presents an assessment of the absorption kinetics, structural, tribological, durability of polymer-enhanced mucin films and their ability to reduce the occurrence of material wear, there are a number of limitations. Firstly, the choice of absorption substrate must be considered. In this study, the Au QCM sensors and *Y*-TZP ceramic as the tribo-couple were used. This enabled a fundamental and direct correlation between absorbed film and tribological properties possible. These are common biomaterials used within the oral environment, particularly in hard-hard interfaces such as artificial/replacement teeth and amalgam applications. To enable translation of any dry mouth technology to clinical application, future work should consider physiologically representative surfaces and other interfaces found within the oral environment (e.g., natural and synthetic biomaterials

including teeth ($CaPO_4$) and soft tissue). Secondly, the conditions under which these films are tested also need to be considered. It has been shown that the films formed have the potential to reduce wear of Au surface incurred through tribological interactions. However, it is well established that oral surfaces are subjected to a wide range of environmental conditions that subsequently affect surface degradation [5]. As such, the long-term durability of these surface layers needs to be considered under a range of adverse, but physiologically relevant, environmental conditions. Nonetheless, the ability to engineer durable and stable mucin films that have the potential to mitigate wear occuring at tribological contacts within the oral environment has significant benefits in decreasing tooth wear and erosion (dissolution).

## 4 Conclusions

Mucin and Polyethylene glycol (PEG) molecules could adsorb onto Au sensors immediately to form soft layers in nanoscale. The chemisorption played a dominant role in the process of mucin/thiolated polyethylene glycol (PEG-SH) adsorption. Meanwhile, the chemical interaction between mucin and PEG-SH molecules promoted the formation of a mixed layer with a three-dimensional network structure, where mucin molecules functioned as a mucoadhesion agent. All the pre-formed layers could decrease friction and wear, especially mucin and PEG-SH mixed layer. Further investigations implied that PEG-SH molecules could interpenetrate into the mucin layer by diffusion and facilitate mucoadhesion to stabilize themselves to decrease friction. The friction-reducing effect of PEG/mucin molecules and the mucoadhesion of mucin contribute to a better lubrication effect of the mixed layer with long effectiveness. This study provided an effective combination to develop long-effective saliva substitutes, where PEG-SH is a lubricating agent while traditional lubricating agent mucin is a mucoadhesion material.

## Acknowledgements

This work was supported by the International Postdoctoral Exchange Fellowship Program (Grant No. 20190060).

**Electronic Supplementary Material:** Supplementary material is available in the online version of this article at https://doi.org/10.1007/s40544-022-0629-2.



## References

[1] Wan H, Vissink A, Sharma P K. Enhancement in xerostomia patient salivary lubrication using a mucoadhesive. *J Dent Res* **99**: 914–921 (2020)

[2] Xu F, Laguna L, Sarkar A. Aging-related changes in quantity and quality of saliva: Where do we stand in our understanding? *J Texture Stud* **50**: 27–35 (2019)

[3] Vinke J, Kaper H J, Vissink A, Sharma P K. Dry mouth: Saliva substitutes which adsorb and modify existing salivary condition films improve oral lubrication. *Clin Oral Invest* **24**: 4019–4030 (2020)

[4] Wan H, Ma C, Vinke J, Vissink A, Herrmann A, Sharma P K. Next generation salivary lubrication enhancer derived from recombinant supercharged polypeptides for xerostomia. *ACS Appl Mater Interfaces* **12**: 34524–34535 (2020)

[5] Smart P, Neville A, Bryant M. Tribocorrosion of dental tissues: The role of mucin. *Tribol Int* **148**: 106337 (2020)

[6] Yakubov G E, Macakova L, Wilson S, Windust J H C, Stokes J R. Aqueous lubrication by fractionated salivary proteins: Synergistic interaction of mucin polymer brush with low molecular weight macromolecules. *Tribol Int* **89**: 34–45 (2015)

[7] Rondelli V, Cola E D, Koutsioubas A, Alongi J, Ferruti P, Ranucci E, Brocca P. Mucin thin layers: A model for mucus-covered tissues. *Int J Mol Sci* **20**(15): 3712 (2019)

[8] Castro I, Sepulveda D, Cortes J, Quest A F, Barrera M J, Bahamondes V, Aguilera S, Urzua U, Alliende C, Molina C, et al. Oral dryness in Sjogren's syndrome patients. Not just a question of water. *Autoimmun rev* **12**: 567–574 (2013)

[9] Zeng Q, Zheng L, Zhou J, Xiao H, Zheng J, Zhou Z. Effect of alcohol stimulation on salivary pellicle formation on human tooth enamel surface and its lubricating performance. *J Mech Behav Biomed Mater* **75**: 567–573 (2017)

[10] Song J, Lutz T M, Lang N, Lieleg O. Bioinspired dopamine/mucin coatings provide lubricity, wear protection, and cell-repellent properties for medical applications. *Adv Healthc Mater* **10**: e2000831 (2021)

[11] Marczynski M, Jiang K, Blakeley M, Srivastava V, Vilaplana F, Crouzier T, Lieleg O. Structural alterations of mucins are associated with losses in functionality. *Biomacromolecules* **22**: 1600–1613 (2021)

[12] Jiang K, Yan H, Rickert C, Marczynski M, Sixtensson K, Vilaplana F, Lieleg O, Crouzier T. Modulating the bioactivity of mucin hydrogels with crosslinking architecture. *Adv Funct Mater* **31**: 2008428 (2021)

[13] Petrou G, Crouzier T. Mucins as multifunctional building blocks of biomaterials. *Biomater Sci* **6**: 2282–2297 (2018)

[14] Shetty P, Mu L, Shi Y. Polyelectrolyte cellulose gel with PEG/water: Toward fully green lubricating grease. *Carbohydr Polym* **230**: 115670 (2020)

[15] Hu J, Andablo-Reyes E, Mighell A, Pavitt S, Sarkar A. Dry mouth diagnosis and saliva substitutes-A review from a textural perspective. *J Texture Stud* **52**: 141–156 (2021)

[16] Pailler-Mattei C, Vargiolu R, Tupin S, Zahouani H. Ex vivo approach to studying bio-adhesive and tribological properties of artificial salivas for oral dryness (xerostomia). *Wear* **332–333**: 710–714 (2015)

[17] Kane S R, Ashby P D, Pruitt L A. Characterization and tribology of PEG-like coatings on UHMWPE for total hip replacements. *J Biomed Mater Res A* **92**: 1500–1509 (2010)

[18] Han T, Yi S, Zhang C, Li J, Chen X, Luo J, Banquy X. Superlubrication obtained with mixtures of hydrated ions and polyethylene glycol solutions in the mixed and hydrodynamic lubrication regimes. *J Colloid Interface Sci* **579**: 479–488 (2020)

[19] Kobayashi M, Koide T, Hyon S H. Tribological characteristics of polyethylene glycol (PEG) as a lubricant for wear resistance of ultra-high-molecular-weight polyethylene (UHMWPE) in artificial knee join. *J Mech Behav Biomed Mater* **38**: 33–38 (2014)

[20] Sang T, Ye Z, Fischer N G, Skoe E P, Echeverria C, Wu J, Aparicio C. Physical-chemical interactions between dental materials surface, salivary pellicle and Streptococcus gordonii. *Colloid Surf B* **190**: 110938 (2020)

[21] Barrantes A, Arnebrant T, Lindh L. Characteristics of saliva films adsorbed onto different dental materials studied by QCM-D. *Colloid Surf A* **442**: 56–62 (2014)

[22] Yakubov G E, McColl J, Bongaerts J H H, Ramsden J J. Viscous boundary lubrication of hydrophobic surfaces by mucin. *Langmuir* **25**: 2313–2321 (2009)

[23] Oh S, Borros S. Mucoadhesion vs mucus permeability of thiolated chitosan polymers and their resulting nanoparticles using a quartz crystal microbalance with dissipation (QCM-D). *Colloid Surf B* **147**: 434–441 (2016)

[24] Xu F, Liamas E, Bryant M, Adedeji A F, Andablo‐Reyes E, Castronovo M, Ettelaie R, Charpentier T V J, Sarkar A. A self‐assembled binary protein model explains high‐performance salivary lubrication from macro to nanoscale. *Adv Mater Interfaces* **7**: 1901549 (2019)

[25] Clear S C, Nealey P F. Chemical force microscopy study of adhesion and friction between surfaces functionalized with self-assembled monolayers and immersed in solvents. *J Colloid Interface Sci* **213**: 238–250 (1999)

[26] Lee J. Nanoscopic friction behavior of pharmaceutical materials. *Int J Pharm* **340**: 191–197 (2007)

[27] Lanigan J L, Fatima S, Charpentier T V, Neville A, Dowson D, Bryant M. Lubricious ionic polymer brush functionalised silicone elastomer surfaces. *Biotribology* **16**: 1–9 (2018)

[28] Macakova L, Yakubov G E, Plunkett M A, Stokes J R. Influence of ionic strength changes on the structure of pre-adsorbed salivary films. A response of a natural multi-component layer. *Colloid Surf B* **77**: 31–39 (2010)

[29] Oh S, Wilcox M, Pearson J P, Borros S. Optimal design for studying mucoadhesive polymers interaction with gastric mucin using a quartz crystal microbalance with dissipation (QCM-D): Comparison of two different mucin origins. *Eur J Pharm Biopharm* **96**: 477–483 (2015)

[30] Simonin J-P. On the comparison of pseudo-first order and pseudo-second order rate laws in the modeling of adsorption kinetics. *Chem Eng J* **300**: 254–263 (2016)

[31] Alkan M, Demirbaş Ö, Doğan M, Arslan O. Surface properties of bovine serum albumin–adsorbed oxides: Adsorption, adsorption kinetics and electrokinetic properties. *Micropor Mesopor Mater* **96**: 331–340 (2006)

[32] Ho YS. Review of second-order models for adsorption systems. *J Hazard Mater* **136**: 681–689 (2006)

[33] Marczynski M, Balzer B N, Jiang K, Lutz T M, Crouzier T, Lieleg O. Charged glycan residues critically contribute to the adsorption and lubricity of mucins. *Colloid Surf B* **187**: 110614 (2020)

[34] Kitano H, Hayashi A, Takakura H, Suzuki H, Kanayama N, Saruwatari Y. Anti-biofouling properties of a telomer brush with

pendent glucosylurea groups. *Langmuir* **25**: 9361–9368 (2009)
[35] He X, Liu Y, Bai X, Yuan C, Li H. Alginate/albumin in incubation solution mediates the adhesion and biofilm formation of typical marine bacteria and algae. *Biochem Eng J* **139**: 25–32 (2018)
[36] Sajewicz E. Effect of saliva viscosity on tribological behaviour of tooth enamel. *Tribol Int* **42**: 327–332 (2009)
[37] Klein J. Hydration lubrication. *Friction* **1**: 1–23 (2013)
[38] Information on https://bnf.nice.org.uk/clinical-medical-device-information-group/as-saliva-orthana-spray.html.

**Xiaoyan HE.** She received her bachelor degree in materials science and engineering in 2012 from Huazhong University of Science and Technology, Wuhan, China. Then, she obtained her Ph.D. degree in materials physics and chemistry in 2017 from University of Chinese Academy of Sciences, China. She joined Wuhan University of Technology from 2017. Her research interests include tribology of biomolecules, biofouling, and biocorrsion.

**Michael BRYANT.** He received his B.Eng. (hons) and Ph.D. degrees in mechanical engineering from the University of Leeds, UK, in 2010 and 2013, respectively. After a short time at DePuy International, he joined the Institute of Functional Surfaces at the University of Leeds in 2015. He is currently an associate professor of Tribology and Corrosion Engineering. His research areas cover the tribology and corrosion of a variety of materials for biomedical applications, both hard and soft.